ResearchGate

See discussions, stats, and author profiles for this publication at: https://www.researchgate.net/publication/273833786

Water-Mediated Differential Binding of Strontium and Cesium Cations in Fulvic Acid

ARTICLE *in* THE JOURNAL OF PHYSICAL CHEMISTRY B · MARCH 2015

Impact Factor: 3.3 · DOI: 10.1021/acs.jpcb.5b01659 · Source: PubMed

CITATIONS
2

READS
19

3 AUTHORS, INCLUDING:

Biswajit Sadhu
Bhabha Atomic Research Centre
10 PUBLICATIONS **21** CITATIONS
SEE PROFILE

Mahesh Sundararajan
Department of Atomic Energy
56 PUBLICATIONS **535** CITATIONS
SEE PROFILE

Available from: Biswajit Sadhu
Retrieved on: 25 January 2016

THE JOURNAL OF PHYSICAL CHEMISTRY B

Article

pubs.acs.org/JPCB

Water-Mediated Differential Binding of Strontium and Cesium Cations in Fulvic Acid

Biswajit Sadhu,[†] Mahesh Sundararajan,*[,‡] and Tusar Bandyopadhyay*[,‡]

[†]Radiation Safety Systems Division, Bhabha Atomic Research Centre, Mumbai 400 085, India

[‡]Theoretical Chemistry Section, Bhabha Atomic Research Centre, Mumbai 400 085, India

Supporting Information

ABSTRACT: The migration of potentially harmful radionuclides, such as cesium (^{137}Cs) and strontium (^{90}Sr), in soil is governed by the chemical and biological reactivity of soil components. Soil organic matter (SOM) that can be modeled through fulvic acid (FA) is known to alter the mobility of radionuclide cations, Cs^+ and Sr^{2+}. Shedding light on the possible interaction mechanisms at the atomic level of these two ions with FA is thus vital to explain their transport behavior and for the design of new ligands for the efficient extraction of radionuclides. Here we have performed molecular dynamics, metadynamics simulations, and density-functional-theory-based calculations to understand the binding mechanism of Sr^{2+} and Cs^+ cations with FA. Our studies predict that interaction of Cs^+ to FA is very weak as compared with Sr^{2+}. While the water−FA interaction is largely responsible for the weak binding of Cs^+ to FA, leading to the outer sphere complexation of the ion with FA, the interaction between Sr^{2+} and FA is stronger and thus can surpass the existing secondary nonbonding interaction between coordinated waters and FA, leading to inner sphere complexation of the ion with FA. We also find that entropy plays a dominant role for Cs^+ binding to FA, whereas Sr^{2+} binding is an enthalpy-driven process. Our predicted results are found to be in excellent agreement with the available experimental data on complexation of Cs^+ and Sr^{2+} with SOM.

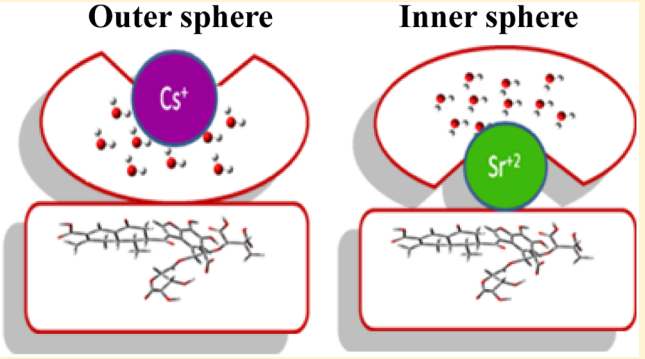

1. INTRODUCTION

Once they are released into the environment, long-lived radioactive fission products such as ^{137}Cs and ^{90}Sr can present a potential biological threat to human health.[1] The dominant sources for these releases are from nuclear reactor accidents,[2] nuclear weapon tests,[3] fuel reprocessing plants, and so on.[4,5] Being radioactive in nature, handlings of these two radionuclides require extra safety precautions in the case of experimental studies. These radionuclides, once deposited onto the soil, can further react with the first layer of soil, which generally contains a large amount of soil organic matter (SOM). Humic acid (HA) and fulvic acid (FA) are major components of SOM. Both HA and FA contain various functional groups such as carboxyl, quinone, and phenolate, which can bind various radionuclides,[6] restricting the mobility of these ions in soil environment depending on the water content, pH, and ionic strengths of the acids.[7,8]

Most of the experimental studies are focused to evaluate SOM influence on radionuclide sorption into mineral layers,[9−12] while experiments on the direct interaction of Cs^+ and Sr^{2+} with FA are limited.[13] Nevertheless, these studies perceived the vital role of SOM on radionuclide mobility. For example, Staunton et al.[14] observed enhanced absorption of cesium into montmorillonite and illite mineral surfaces in the presence of FA.[15] Furthermore, similar chemical properties of its group congeners (K^+ and Ca^{2+}) are suggestive of the fact that Cs^+ and Sr^{2+} might also be absorbed by plants and enter into the human food chains.[16,17] For instance, Sanchez et al.[18] observed that a significant amount of Cs^+ is absorbed by plants in organic soil, whereas the Sr^{2+} uptake in plants was observed to be minimal.[19] Apart from this, several data fitting semiempirical models were also proposed to understand the metal−SOM interactions.[20,21] The accuracy of such modeling approach is metal-specific and depends on the availability of experimentally derived parameters.[22]

Powerful theoretical methods such as quantum mechanics (QM) and molecular dynamics (MD) can provide valuable information on the structures, conformational flexibility, and cation binding affinities of SOM at the molecular level;[23,24] however, only a few of computational studies have been carried out due to uncertainty in the structure of FA.[25] Of the various possible FA models, the Leenheer[26] model is considered to be one of the realistic models that possess essential functional groups present in FA. Trout and Kubicki[27] have calculated the

Special Issue: Biman Bagchi Festschrift

Received: February 18, 2015
Revised: March 18, 2015

ACS Publications © XXXX American Chemical Society

DOI: 10.1021/acs.jpcb.5b01659
J. Phys. Chem. B XXXX, XXX, XXX−XXX

proton and guest affinities of carboxylate functional groups using the Leenheer model.[28] Burk et al.[29] and Mayeux et al.[30] have calculated the Cs^+ binding affinity to several isolated functional groups of SOM in gas phase. In both studies, the effect of solvents was not considered, which may not reflect the true binding affinities as in realistic SOM. The influence of water molecules on the binding affinities of several multivalent cations to SOM was investigated by Aquino et al.[31−33] using classical MD simulations. Recently, we have investigated structures and possible binding motifs of uranyl ion to HA and FA models using a combined density-functional-theory (DFT)- and MD-based calculations.[34] In line with Aquino et al.,[31−33] we have also emphasized the importance of incorporating solvents effects and neighboring groups, which can modulate the binding affinities of the actinide ion. A combination of different theoretical methods can be extremely useful to tackle the challenging speciation issue of radionuclides in SOM. Note that the use of QM alone can accurately describe the static picture and to some extent the structural conformations using the ab initio molecular dynamics (AIMD) simulations with limited system size and time scale. Similarly, classical MD and its nonequilibrium counterpart, metadynamics (MtD),[35,36] can provide valuable information on dynamical behavior of the system and can treat significantly bigger systems with larger time scale quite efficiently.

Here we present a systematic theoretical approach that applies all three of these methods (MtD, MD, and QM) to explore the binding mechanism of Cs^+ and Sr^{2+} to FA in the presence of explicit water molecules. We choose FA model to represent SOM because of its higher reactivity as compared with HA.[6] Our strategy is as follows. We first carried out a set of DFT calculations to find the most probable binding site of FA, interacting with radionuclides. The resulting FA structure is then embedded in explicit water. Complexing ion (Cs^+ or Sr^{2+}) is added and the system is equilibrated through classical MD simulation. MtD is then used to find the stationary points in the free-energy landscape of FA−water−ion complexes. MD simulations and QM calculations are carried out on the MtD extracted structures to understand the speciation and binding preferences of Cs^+ and Sr^{2+} to FA. Finally, we arrive at a differential binding mechanism between the two radionuclide ions with SOM, mediated by the intervening water molecules.

2. COMPUTATIONAL METHODS

Quantum-Mechanical Study. The chosen FA model contains four carboxylic acid groups (denoted as 'A', 'B', 'C', and 'D' in Figure 1), quinone, phenolic hydroxo groups, and heterocyclic rings, which are the minimum prerequisites for a FA model. The starting structure is taken from Trout and Kubicki.[27] For geometry optimizations, we have used a dispersion-corrected BP86 functional[37,38] with def2-SV(P)[39] basis set. This combination is observed to predict accurate geometries.[34,40−42] To speed up the calculation, we invoked a resolution of identity (RI) approximation for coulomb exchange integrals using a corresponding auxiliary basis set (def2-SV(P)/J). For energetics, a dispersion-corrected B3LYP functional[43,44] with TZVP basis set[45,46] is used. For both Cs^+ and Sr^{2+}cations, a def2-SV(P) (for geometry optimizations) and def-TZVP basis set were used to describe the valence orbitals, whereas the core orbitals were modeled via def-ECP (contains 46 core electrons for cesium, 28 electrons for strontium) pseudopotential. The influence of larger basis set TZVP on the structures is found to be minimal (Supporting Information, Table S1). Changing from double-ζ to triple-ζ basis set, we find little change in the computed structures. Hence, throughout the study, medium-sized basis set is used for geometry optimization. Long-range electrostatic interactions are accounted for by the COSMO continuum solvation model[47] for both of the geometry optimizations and as well as the energy evaluations. In these calculations, the dielectric constant (ϵ = 80) of water is used to mimic the solvent effect, as implemented in Turbomole (Turbomole V6.3 2011).[48] Harmonic frequency calculations are performed using the AOFORCE module to identify the species at minima and for thermodynamic properties. Thermodynamic quantities such as change of enthalpy (ΔH), entropy (ΔS), and Gibbs free energies (ΔG) for the complexation are derived from FREEH module.

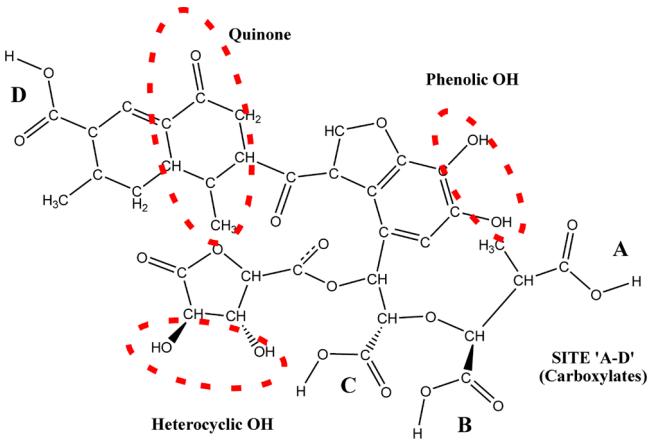

Figure 1. Model structure of FA showing the presence of various functional groups.

Proton affinities of carboxylate functional groups of FA ($FA^{-1} + H_3O^+ \rightarrow FA + H_2O$) and subsequent ion binding energies (ΔE) of FA^{-1} with $[FA^{-1} + M(H_2O)_n^{+/2+} \rightarrow FA{-}M{-}(H_2O)_m^{0/+} + (H_2O)_k$ for M = Cs^+/Sr^{2+}] are calculated using the following equations.

$$\text{proton affinity} = [E(\text{FA}) + E(\text{H}_2\text{O})] - [E(\text{FA}^{-1}) + E(\text{H}_3\text{O}^+)] \quad (1)$$

$$\Delta E = (E[\text{FA}{-}\text{M}(\text{H}_2\text{O})_m]^{0/+} + E[(\text{H}_2\text{O})_k]) - (E[\text{FA}^{-1}] + E[\text{M}(\text{H}_2\text{O})_n]^{+/2+}) \quad (2)$$

where n and m are the number of water molecules in the metal−hydrate and FA−metal−water systems, respectively. k is the number of water molecules released during binding reaction. These numbers are evaluated through MD and subsequent DFT level calculations. (See later.) Natural population analysis[49] (NPA) scheme is used to quantify the charge transfer from metal to FA and water molecules upon complexation. The effects of other density functionals on the computed binding energetics of the radionuclides to FA are carried out using ORCA 3.0.[50]

MD Simulation. All MD simulations are carried out using GROMACS 4.5.4 package.[51] The required force-field parameters of Cs^+ and Sr^{2+}ions are taken from Aqvist et al.[52] and Larentzos et al.,[53] respectively. Partial atomic charges are further modified using the charges derived from the NPA scheme.[49] Force-field parameters of FA are determined using the ANTECHAMBER[54] module based on the general amber

DOI: 10.1021/acs.jpcb.5b01659
J. Phys. Chem. B XXXX, XXX, XXX−XXX

force field (GAFF).[55] FA is solvated in a box of size 4 × 4 × 4 nm^3 containing 2141 TIP3P[56] water molecules. FA is equilibrated after successive steps of energy minimization (steepest descent method) and position restrained simulations for 800 ps by allowing movement of water molecules around FA. The systems (FA, water, and metal ion) are kept at a fixed temperature of 300 K via V-rescale thermostat.[57] For long-range electrostatic interaction, particle mesh Ewald (PME)[58] sums are used, while the LINCS algorithm[59] is followed to constrain bonds between hydrogen and the heavy atoms at their equilibrium lengths. For short-range electrostatic and van der Waals interaction, a cut off of 14 Å is applied. Finally, during 10 ns equilibration period, equation of motion is integrated with 2 fs time step. Purposefully, for the cation containing systems, cations are kept 8 Å away from the most preferable binding site of FA, ensuring no interaction between them.[60] The equilibrated structures are then used as the starting configuration for MtD simulations. (See later.) Next, we have carried out classical MD simulations for another 5 ns on the MtD extracted structures of the ion−FA complexes. The choice of cation-bound FA structures for the final MD simulations is based on the free-energy landscape obtained from MtD simulations.

In addition, conformational entropy is calculated based on the well-known Schlitter's method,[61] which provides an approximate upper bound of conformational entropy, S

$$S < S_{\text{Schlitter}} = \frac{1}{2}k_{\text{B}}T \ln \det\left[1 + \frac{k_{\text{B}}Te^2}{\hbar^2}M\sigma\right] \quad (3)$$

where k_{B} is Boltzmann's constant, e is Euler's number, $\hbar$ is Planck's constant divided by 2π, T is absolute temperature, M is the 3D diagonal matrix consisting of N atomic masses of solute atoms for which the entropy is calculated, and σ is the covariance matrix to take care of atom positional fluctuations and is represented by

$$\sigma_{ij} = \langle (x_i - \langle x_i \rangle)(x_j - \langle x_j \rangle) \rangle \quad (4)$$

where x_i is the Cartesian coordinate of the atom i.

Metadynamics Simulation. We have employed MtD method[62] to enforce the migration of cation toward FA by adding to the potential well a time-dependent external biased potential (V_{MtD}) along a chosen set of collective variables (CVs). V_{MtD} is a construct of Gaussian hills with height, H, and width, w, that are added at a time interval, τ_{G}, so as to overcome the free-energy barrier associated with local minima, which eventually leads to exploration of more configuration space in a relatively short time. Finally, the resulted potential enables one to reconstruct the free-energy landscape for the system without any prior assumption. Details of this method can be found elsewhere.[63] Two CVs, namely, hydration number of the ion and the distance of the ion with respect to the center of mass (COM) of the system, are taken to construct 2D free-energy surface (2D FES) landscape. The rapid search of local minima in FES depends on the values of H and w. As experimental hydration energy of Sr^{2+}(∼ −330 kcal mol^{-1}) is roughly six times higher compared with Cs^+(∼ −59 kcal mol^{-1}),[64] smaller Gaussian height is applied for Cs^+ (0.05 kcal mol^{-1}) as compared with Sr^{2+}(0.1 kcal mol^{-1}), while Gaussian width (w) of 0.25 is used for both the cations. Gaussians are added after every picosecond. Finally, systems are subjected to production run of 100 ns with trajectories being saved every 1 ps for further analysis. FES profiles are explored from the deposited Gaussian. All MtD simulations are performed using PLUMED 1.3[65] patch to the GROMACS software package.

3. RESULTS AND DISCUSSION

Solvation of Cs^+ and Sr^{2+} Ions. The hydration free energy of radionuclide ions plays a vital role for the effective binding of radionuclide with FA. Several experiments[66−69] and electronic structure calculations[70−72] have predicted that the hydration number of Sr^{2+} and Cs^+ varies from six to eight water molecules. In particular, Ali and coworkers[71,72] have reported that eight water molecules can directly coordinate to Sr^{2+}, whereas partial solvation of up to six water molecules to Cs^+ is noted.

We have calculated the hydration number ($N(r)$) of both of the cations using the radial distribution function (RDF) using equilibrium MD (Figure 2). The RDF profile for Sr^{2+} shows a

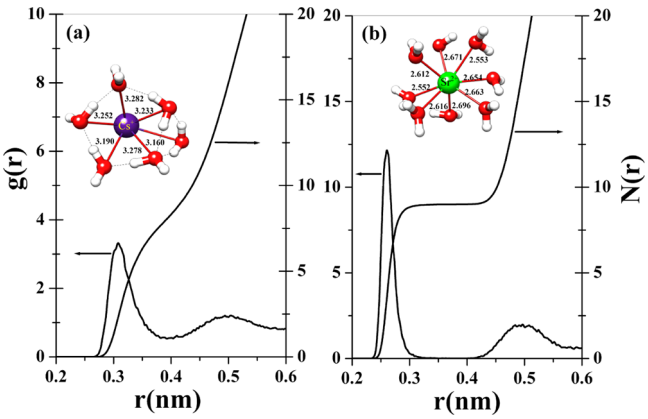

Figure 2. Radial distribution functions, $g(r)$, and corresponding integrals, $N(r)$, of (a) Cs^+ and (b) Sr^{2+} with respect to oxygen atom of water molecules. Structure of metal−hydrate systems as extracted from the plateau region of the $N(r)$ plots and optimized at BP86/def2-SV(P) level are shown in the inset.

sharp first peak at 2.62 Å, and it is separated by depletion zone, confirming the stability of first hydration shell. In contrast with Sr^{2+}, the RDF profile of Cs^+ indicates a relatively broad peak at 3.10 Å, which corresponds to closest Cs−O separation. Clearly, hydration shell around Cs^+ is relatively weaker. From the RDF profile we found that the first hydration shell of Cs^+ and Sr^{2+} contains six and eight water molecules, respectively. Thus, while calculating ion binding free energies using eq 2, we took n = 6 and 8 for Cs^+ and Sr^{2+}, respectively. The hydrated metal ion structures [$Cs(H_2O)_6^+$ and $Sr(H_2O)_8^{2+}$] were extracted from the MD trajectories (after 10 ns of equilibration period) and optimized at the DFT level [(BP86/def2-SV(P)]. Optimized hydrated metal ions indicate that water molecules around Sr^{2+} are more rigid as compared with Cs^+. Furthermore, we find that water molecules around Cs^+ form an asymmetric hydrated structure[73] (Cs^+−O_{water}, 3.160−3.282 Å), whereas for Sr^{2+} the water molecules remain strongly coordinated (Sr^{2+}−O_{water}, 2.552−2.696 Å) to ion (Figure 2). Our optimized radionuclide−water bond lengths are in excellent agreement with the previously reported computational study (Cs^+−O_{water}, 3.25 Å;[74] Sr^{2+}−O_{water}, 2.56−2.61 Å[71]) and with available XAFS data[69]-(Sr^{2+}−O_{water}, 2.60 Å). Furthermore, the calculated hydration free energies for Cs^+ (−47.1 kcal mol^{-1}) are somewhat underestimated (by 10 kcal mol^{-1}) as compared with experimental data,[64] whereas for Sr^{2+} (−338.3 kcal mol^{-1}),

DOI: 10.1021/acs.jpcb.5b01659
J. Phys. Chem. B XXXX, XXX, XXX−XXX

the calculated value is overestimated by 8 kcal mol^{-1} (Supporting Information, Table S2). Nevertheless, our calculated hydration free energies of both the metals are observed to follow the experimental trend closely.

Structure and Proton Affinities of FA. As previously mentioned, the chosen FA model has four carboxylic acid functional groups, which are denoted as 'A', 'B', 'C', and 'D' (cf. Figure 1). Our optimized geometric parameters for the functional groups in the FA model are closer to the experimental data.[75,76] The computed asymmetric stretching frequencies (ν_{asym}) for the various functional groups present in FA are comparable to experimental IR data (Supporting Information, Table S3).[77]

The pK_a of the carboxylic acid functional group varies from 2 to 4 in FA at the physiological pH.[26] Thus, at the neutral pH range, the carboxylic acid group is expected to deprotonate first as compared with hydroxyl functional group (pK_a = 6−8). Single deprotonation of carboxylic acid groups at various sites led to four anionic FA models, denoted by FA (N), where N refers to various deprotonated carboxylate site, that is, in Figure 1A−D. Notably, the four carboxylic groups of FA do not have the same chemical environment. Proton affinity values presented in Table 1 show that among the four possible deprotonated sites we find that FA(C) is the most stable structure (by 5 kcal mol^{-1} with respect to FA(D)). In FA (C) structure, the negative charge of carboxylate 'C' group is delocalized due to the presence of electronegative ether group near to it. It is evident from the structure in Figure 1 that the nearby heterocyclic OH group interacts strongly via hydrogen bonding (1.49 Å) with the deprotonated carboxylate group. The negative charges created by deprotonating at sites "B' or 'D" sites is not stabilized by the neighboring groups as compared to "C' or 'A" site. Thus, the calculated relative energies follows the order, FA(C) > FA(A) > FA(B) > FA(D), which are consistent with the experimental observation of Leenheer et al.[26] (Table 1). Similar to relative energetics, our calculated proton affinity of different deprotonated structures also suggests that the 'C' site in FA is the most stable structure having the lowest proton affinity value (−31.70 kcal mol^{-1}). Thus, at physiological pH (pH ∼7), the FA(C) site remains deprotonated, which can bind Cs^+ or Sr^{2+} radionuclide. Hereafter, for simplicity, FA (C) will be represented as FA.

Table 1. Calculated Proton Affinities and Relative Energies (kcal mol^{-1}) of FA at Different Deprotonated States

FA	proton affinity	relative energy
FA (A)	−34.1	+2.43
FA (B)	−36.3	+4.56
FA (C)	−31.7	0.00
FA (D)	−36.9	+5.42

Binding of Radionuclides to FA. Later we first obtain the possible structure of FA bound radionuclide ions in explicit water solvent through the search of local minima of ion−FA interacting system using metadynamics simulation. The structures deduced from MtD simulation are then utilized in equilibrium MD simulation and DFT calculation to shed light into the differential binding of the two ions with FA.

MtD Simulation. A 100 ns MtD simulation trajectory reveals that Cs^+ is dominantly found near the bulk water at a distance of 6 to 7 Å from the 'C' site of FA; however, Cs^+, intermittently for short duration of time, is also found near carboxylate and heterocyclic OH binding sites of FA (Supporting Information, Figure S1). In the FES plot presented in Figure 3, we find a broad blue region around 6 Å away from the 'C' site of FA, indicating a global minima away from FA. This suggests that interaction of Cs^+ with FA is rather weak and water−FA interaction dominates over Cs^+−FA interaction. On the contrary, Sr^{2+} is frequently observed to come closer and remain bound to FA for longer duration (5−10 ns, Figure S1 in the Supporting Information), resulting in the formation of free-energy minimum near to FA. For Sr^{2+}, the local minima are tilted toward the carboxylate of FA, suggesting that the interaction is strong with FA.

To understand the nature of binding pattern and mechanism, we have analyzed the individual interactions of the two radionuclides with FA and water. The change of average interaction energy with respect to COM separation between radionuclide ions and FA is shown in Figure 4. It is quite evident that all three components (ion−water, water−FA, and ion−FA) contribute to the average interaction energy significantly. As Sr^{2+} approaches the 'C' site of FA, the Sr^{2+}−water and FA−water interaction energy decrease (becomes more positive), which is compensated by the favorable interaction energy between FA−Sr^{2+} (more negative). These are largely due to the shedding of water molecules from solvation shells of ion and FA, which gives rise to less negative

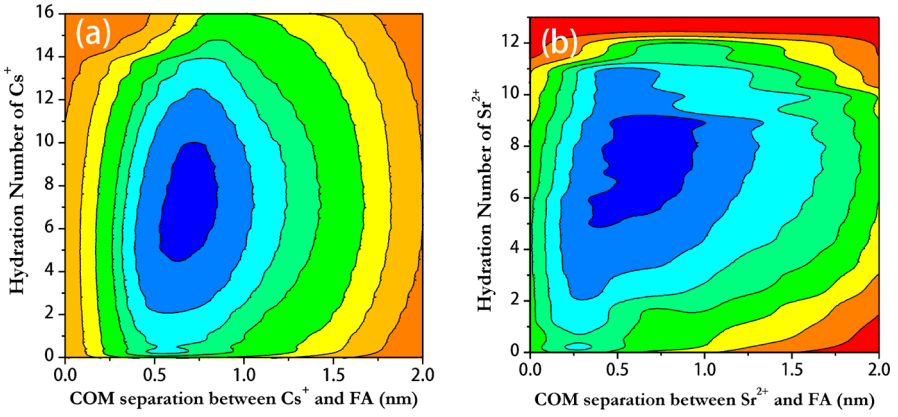

Figure 3. Free-energy landscapes of (a) Cs−FA and (b) Sr−FA complexes obtained from MtD simulations. Free energy is plotted as a function of hydration number of the ions and their separation from the center of mass (COM) of the binding site 'C' of FA. Energy increases from blue to red in the free-energy landscape. Cation-bound FA structures are extracted from the energy minima and are further subjected to MD and QM calculations.

DOI: 10.1021/acs.jpcb.5b01659
J. Phys. Chem. B XXXX, XXX, XXX−XXX

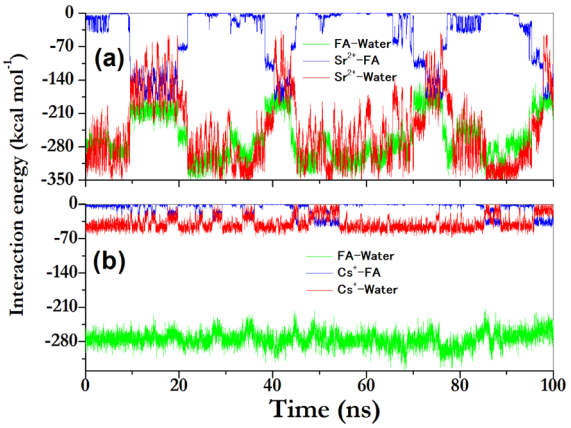

Figure 4. Interaction energies for (a) Sr^{2+} and (b) Cs^{+} during 100 ns MtD simulations. Ion–water, ion–FA, and FA–water interaction energies are indicated in red, blue, and green, respectively.

interaction energy for Sr^{2+}–water system. Because of the smaller hydration energy of Cs^{+}(−59 kcal mol^{-1}), the shedding of water molecules is more facile as compared with Sr^{2+}.Thus, Cs^{+} is expected to bind FA strongly; however, FA–water interaction energy (∼ −280 kcal mol^{-1}) is much stronger as compared with Cs^{+}–FA interaction energy. This leads to weak binding of Cs^{+} to FA. Sr^{2+}–water and FA–water interaction energies are comparable to each other. Consequently, Sr^{2+} can break the FA–water interaction to bind favorably with FA.

MD Simulation. Our MtD simulations suggest that Cs^{+} is expected to get diffused at the bulk as compared with Sr^{2+}. To evaluate the binding affinities of both the radionuclides toward FA, frequently visited configurations are extracted from MtD trajectory, where cations are found to be bound to FA. A 5 ns equilibrium MD simulation is carried out on these cation-bound FA structures. Note that neighboring hydroxo groups also interact strongly, which influences the binding of ions to FA. To quantify the overall contribution of FA, water, and site 'C' interacting with the ions, we plotted the coordination number (CN) of the ions to these chelating agents with respect to time (picoseconds) in Figure 5. We have considered the

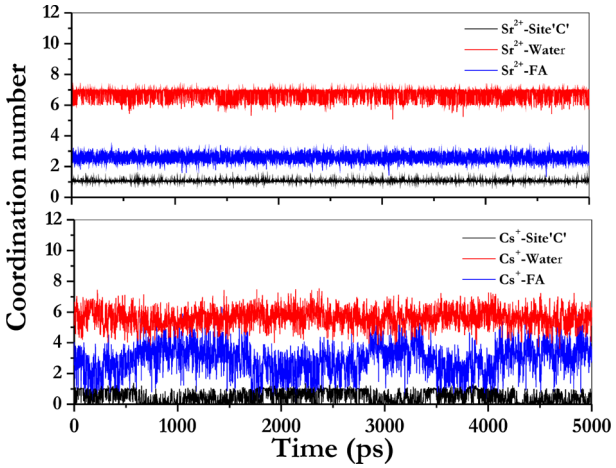

Figure 5. Coordination number for (a) Sr^{2+} and (b) Cs^{+} as a function of time (picoseconds) during equilibrium MD simulation of MtD-extracted FA–ion–water complexes. Ion–water, ion–FA, and ion-site 'C' coordination numbers are shown in red, blue, and black, respectively.

primary coordination shell radius of Cs^{+} to be 3.10 Å and of Sr^{2+} to be 2.62 Å for the simulation. Throughout the simulation, Sr^{2+} hydration number varies from six to seven, whereas for Cs^{+}, it fluctuates between four to six (red line in Figure 5). Furthermore, the carboxylate at site C is monodentate for both Sr^{2+} and Cs^{+} ion (black line in Figure 5). While calculating ion-binding free energies using eq 2, however, we took m = 6 for both of the cations, Cs^{+} and Sr^{2+}. Note that the value of k in eq 2 is now determined as 0 (for Cs^{+}) and 2 (for Sr^{2}).

In Figure 5, because of the influence of neighboring hydroxo group, the CN varies from 1 to 5 for Cs^{+}, whereas it is 2 to 3 for Sr^{2+} (blue line). It is important to mention here that such neighboring group participation could not be observed in the "small" models[29] containing isolated functional group. Furthermore, to assess the diffusiveness of both the metals in the FA–water system, we have calculated the mean-square displacement (MSD) of the ions and found that MSD of Cs^{+} is three times higher as compared with Sr^{2+} (Supporting Information, Figure S2). These variations confirm the higher mobility of Cs^{+} as compared with Sr^{2+}. The favorable binding of radionuclides to FA in the presence of water molecules often depends on entropic factors, where loss of conformational entropy upon interaction leads to unfavorable binding. Figure 6

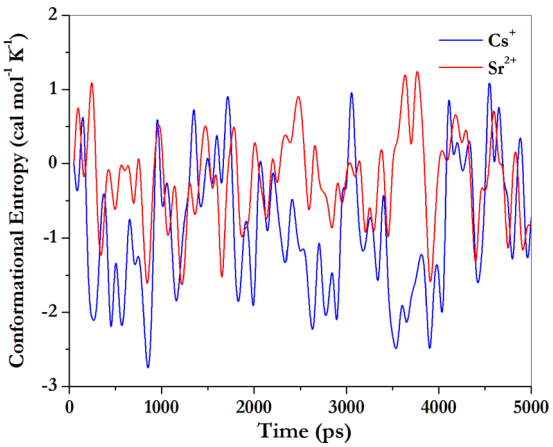

Figure 6. Conformational entropy versus time plot from 5 ns equilibrium run of MtD extracted FA–ion complexes in the presence of water.

shows the calculated conformational entropy. Clearly, Cs–FA system exhibits relatively larger negative entropy values. This is due to favorable FA–water interaction and weak hydration shell of Cs^{+}. For the Sr–FA system, the change of conformational entropy is minimal and fluctuates from −1 to 1 cal mol^{-1} K^{-1}.

DFT Calculation. Figure 7 represents the optimized structures extracted from the MtD trajectory at the BP86/def2-SV(P) level. In our optimized structures, we find that Cs^{+} interacts weakly at the deprotonated site of FA, which is consistent with our MtD and MD simulations. Furthermore, the water molecules are hydrogen-bonded (1.63 to 1.84 Å) with each other and with FA carboxylate functional groups (1.62 to 1.78 Å). We also find that nearby functional groups interact strongly with Cs^{+} ($Cs–O_{ether}$ = 3.177 Å, $Cs–O_{Het}$ = 3.102 Å), which led to asymmetric bidentate binding motif for $Cs–O_{COO}$ (3.258 to 3.330 Å). In Cs^{+}–FA adduct, some of the Cs^{+}–H_2O

DOI: 10.1021/acs.jpcb.5b01659
J. Phys. Chem. B XXXX, XXX, XXX–XXX

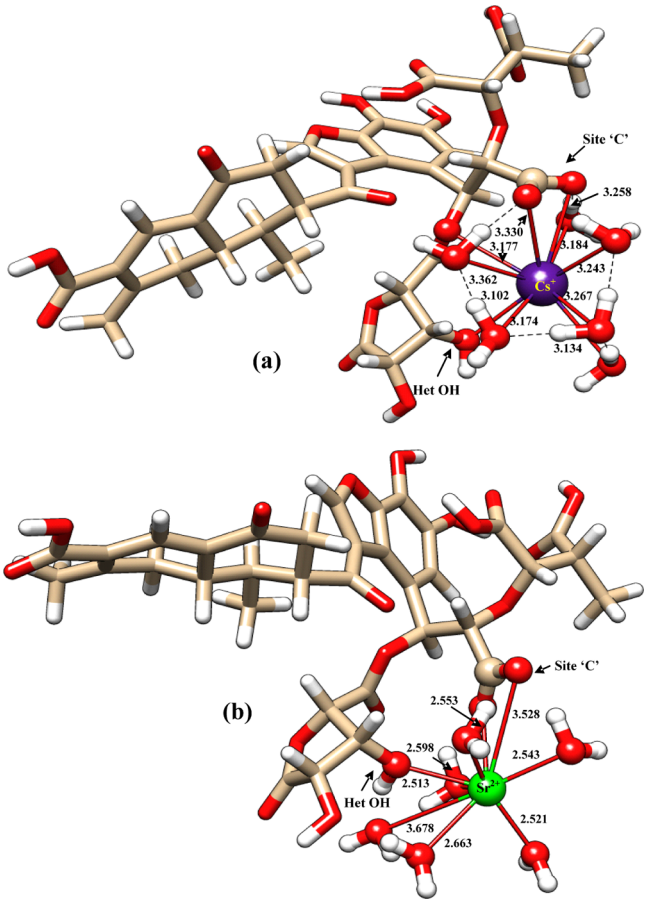

Figure 7. Optimized structure of (a) Cs^+ and (b) Sr^{2+} binding to FA at the 'C' site. Active site coordination and the secondary interactions with FA and water are shown in ball and sticks, whereas the remaining atoms are shown in ball-and-stick frame.

bond lengths are found to be elongated as compared with the bare Cs^+–hydrate structure.

In the case of strontium, an asymmetric monodentate binding motif is noticed for Sr^{2+}–O_{COO} (2.533, 3.528 Å) due to the strong interaction with oxygen of heterocyclic OH functional group (2.513 Å); however, in contrast with Cs^+ binding to FA, water molecules do not solvate the proximal functional groups of FA and mostly remain firmly held by the Sr^{2+}(2.521 Å). This is probably due to the strong hydration energy of Sr^{2+}as compared with Cs^+, which restricts the mobility of water molecules.

Thermodynamic quantities for the ion–FA systems are presented in Table 2. Similar to MD study, binding free energy for Cs^+ with FA is found to be unfavorable (ΔG = +3.88 kcal mol^{-1}), whereas the binding of Sr^{2+} with FA is favorable (−10.40 kcal mol^{-1}). Noticeably, similar formation enthalpies (ΔH) are obtained for both the reactions (∼ −15 kcal mol^{-1}); however, incorporation of entropy effect leads to unfavorable binding of Cs^+. Thus, Cs–FA complexation is entropy-driven, while Sr–FA complexation is enthalpy-driven.

Table 2. Thermodynamic Quantities (kcal mol^{-1}) of Optimized Metal–FA Complexes in FA(C) Model

ion	ΔH	$T\Delta S$	ΔG
Cs^+	−15.32	−19.20	+3.88
Sr^{2+}	−15.50	−5.10	−10.40

Furthermore, the origin of differential binding affinities of the radionuclide cations to FA can be correlated to the extent of charge transfer (see Supporting Information, Table S4) from the radionuclides to FA. We find that the net charge transfer (derived from NPA scheme) from FA to Cs^+ is very small (by ∼0.05 au) as compared with Sr^{2+} (by ∼0.13 au) to FA. Interestingly, coordinating water molecules of Cs^+ are found to be strongly involved in hydrogen bonding with each other and with FA that lead to significantly different charge transfer value (∼ −0.14 au) as compared with water molecules around Sr^{2+} (∼0.02 au) (Figure 7). As previously mentioned, this can be attributed to the smaller hydration energy of Cs^+.

Finally, we have also calculated the binding energies for both the cations with different density functional (DF), such as, M06-2X, M06L, and B97-D3, using optimized structures. Indeed, all DFs predict that Cs^+ binding is unfavorable, whereas Sr^{2+}binding is largely favorable (Table S5 in the Supporting Information). These scrupulous investigations on various aspects lead us to conclude that Cs^+ interacts with FA in an outer sphere binding mechanism, whereas Sr^{2+} binds with FA via inner sphere binding motif.

4. SYNERGY WITH EXPERIMENTS

The molecular level understanding of the speciation of radionuclide Cs^+ and Sr^{2+} cations is investigated through several experimental techniques. Our investigations have addressed various such features, which nicely correlate with the experimental results.

Helal et al.[13] reported that Cs^+ does not form any adduct with FA, whereas Xu et al.[23] reported that only minimal changes are observed in the Cs^{133} chemical shift in the presence of natural organic matter. These studies indicate that Cs^+ interaction with FA is rather weak. In our combined QM, MD, and MtD simulations, we find that the Cs^+ interaction with FA is unfavorable (ΔG_{Cs^+} = ∼4 kcal mol^{-1}), largely due to entropic reasons. Furthermore, the FA–water interactions (∼ −280 kcal mol^{-1}) are very strong as compared with Cs water (−59 kcal mol^{-1}). These findings led us to conclude that Cs binds to FA through outer-sphere mechanism, where the bound water molecules to Cs^+ are interacting with the FA. Thus, water concentration in soil plays a vital role in geochemical environment to form the stable complex with Cs^+. For the case of Sr^{2+} and other alkaline earth metal ions such as Ca^{2+}, experimental studies[24,78] predict strong binding to FA and enthalpy may be the dominant factor.[79] Indeed our calculations predict that Sr^{2+} binding in FA is very strong due to favorable enthalpy factors. Furthermore, the Sr^{2+} cation directly binds with the functional groups of FA, which led us to propose an inner sphere complexation. Although the hydration energy of Sr^{2+} is very large (−330 kcal mol^{-1}), the electrostatic interaction between FA and Sr^{2+} is responsible for the favorable binding of Sr^{2+} to FA. A similar inner sphere binding is also proposed for uranyl binding to HA and FA recently by us.[34]

5. CONCLUSIONS

The speciation and interactions of radionuclides in SOM are important to understand their migration and transport[80,81] into various living organisms such as plants and aquatic species. We have addressed this issue using a variety of tools such as MtD, MD simulations, and DFT-based calculations. Our studies

DOI: 10.1021/acs.jpcb.5b01659
J. Phys. Chem. B XXXX, XXX, XXX–XXX

predict that Cs^+ interacts with SOM through outer sphere pathway and the water molecules play a vital role for the weak binding of Cs^+ to FA. Thus, the increase in water content in soil might lead to Cs^+ being weakly coordinated to FA due to dominant water−FA interactions and form an outer-sphere complex. This binding is energetically unfavorable due to negative entropic contribution, and thus the complex formation is an entropy-driven process. For the Sr^{2+}−FA complex, Sr^{2+} interaction with FA is observed to be favorable because of two contributing factors. Because of high charge by radius ratio, its interaction with functional groups such as carboxylate and hydroxyls is much stronger than that of Cs^+. This also assists us to overcome favorable water−FA interaction via an inner sphere binding motif. Second, contrary to Cs^+−FA system, entropy plays a minor role, and thus complex formation is enthalpy-driven and hence energetically favorable. As an important conclusion, the observed binding mechanism of both of the radionuclides provides probable explanations on the availability of these radionuclides in soil solutions. In the presence of organic matter as the interacting media, we thus expect Cs^+ to remain more mobile and available as compared with Sr^{2+} for further plant uptake or subsequent reactions with mineral layers.[82−86] Hence, SOM can selectively bind Sr^{2+}in the presence of competing radionuclide Cs^+. Here it is important to emphasize that our study does not deal with the effects of competitive binding of other cations like K^+ and Ca^{2+} or the binding via multiple ligands simultaneously, which will certainly complicate the binding mechanism. The work on that direction is currently in progress in our laboratory.

■ ASSOCIATED CONTENT

Supporting Information

Optimized structural parameters, vibrational frequency, hydration free energy, NPA, and binding energy of metal-ion complexes along with two plots concerning MtD and equilibrium simulations. This material is available free of charge via the Internet at http://pubs.acs.org.

■ AUTHOR INFORMATION

Corresponding Authors

*M.S.: Tel: +91 22 2559 0300. Fax: +91 22 2550 5151. E-mail: smahesh@barc.gov.in.

*T.B.: E-mail: btusar@barc.gov.in.

Notes

The authors declare no competing financial interest.

■ ACKNOWLEDGMENTS

M.S. and T.B. thank Dr. B. N. Jagatap for constant encouragement and the BARC computer centre for providing the high performance parallel computing facility (Ameya and Ajeya Systems). B.S. thanks Shri K. Dodiya, Shri R. Singh, Dr. K. S. Pradeepkumar, and Dr. D. N. Sharma for their continuous support and encouragement. M.S. thanks Prof. J. D. Kubicki for providing the semiempirical optimized structure of FA.

■ REFERENCES

(1) Zhu, Y. G.; Shaw, G. Soil contamination with radionuclides and potential remediation. *Chemosphere* **2000**, *41*, 121−128.

(2) Stohl, A.; Seibert, P.; Wotawa, G.; Arnold, D.; Burkhart, J. F.; Eckhardt, S.; Tapia, C.; Vargas, A.; Yasunari, T. J. Xenon-133 and caesium-137 releases into the atmosphere from the Fukushima Daiichi nuclear power plant: determination of the source term, atmospheric dispersion, and deposition. *Atmos. Chem. Phys.* **2011**, *11*, 28319−28394.

(3) Aarkrog, A. The radiological impact of the Chernobyl debris compared with that from nuclear weapons fallout. *J. Environ. Radioact.* **1988**, *6*, 151−162.

(4) Adriano, D. C.; Hoyt, G. D.; Pinder, J. E. Fallout of Cesium-137 on a forest ecosystem in the vicinity of a nuclear fuel reprocessing plant. *Health Phys.* **1981**, *40*, 369−376.

(5) Carlton, H.; Bauer, L. R.; Evans, A. B.; Beary, L. A.; Murphy, C. E.; Pinder, J. E.; Strom, R. N. *Cesium in the Savannah River Site Environment*; WSRC-RP-92-250; Westinghouse Savannah River Company: Aiken, SC, 1992.

(6) Stevenson, F. J. *Humus Chemistry: Genesis, Composition, Reactions*; John Wiley & Sons, Inc.: New York, 1994.

(7) Benedetti, M. F.; Riemsdijk, W. H. V.; Koopal, L. K.; Kinniburgh, D. G.; Gooddy, D. C.; Milne, C. J. Metal ion binding by natural organic matter: From the model to the field. *Geochim. Cosmochim. Acta* **1996**, *60*, 2503−2513.

(8) Sauve, S.; Hendershot, W.; Allen, H. E. Solid-Solution Partitioning of Metals in Contaminated Soils: Dependence on pH, Total Metal Burden, and Organic Matter. *Environ. Sci. Technol.* **2000**, *34*, 1125−1131.

(9) Maguire, S.; Pulford, I. D.; Cook, G. T.; Mackenzie, A. B. Caesium sorptiondesorption in clay-humic acid systems. *J. Soil Sci.* **1992**, *43*, 689−696.

(10) Shaban, I. S.; Macasek, F. Influence of humic substances on sorption of cesium and strontium on montmorillonite. *J. Radioanal. Nucl. Chem.* **1998**, *229*, 73−78.

(11) Hakem, N.; Apps, J. A.; Moridis, G. J.; Al Mahamid, I. Sorption of fission product radionuclides, ^{137}Cs and ^{90}Sr, by Savannah River Site sediments impregnated with colloidal silica. *Radiochim. Acta* **2004**, *92*, 419−432.

(12) Kumar, S.; Tomar, B. S.; Ramanathan, S.; Manchanda, V. K. Effect of humic acid on cesium sorption on silica colloids. *Radiochim. Acta* **2006**, *94*, 369−373.

(13) Helal, A. A.; Arida, H. A.; Rizk, H. E.; Khalifa, S. M. Interaction of cesium with humic materials: A comparative study of radioactivity and ISE measurements. *Radiokhimiya* **2007**, *49*, 458−463.

(14) Staunton, S.; Roubaud, M. Absorption of ^{137}Cs on montmorillonite and Illite: Effect of charge compensating cation, ionic strength, concentration of Cs, K and fulvic acid. *Clays Clay Miner.* **1997**, *45*, 251−260.

(15) Rigol, A.; Vidal, M.; Rauret, G. An overview of the effect of organic matter on soil-radiocaesium interaction: implications in root uptake. *J. Environ. Radioact.* **2002**, *58*, 191−216.

(16) Zhu, Y. G.; Smolders, E. Plant uptake of radiocesium: a review of mechanisms, regulations and application. *J. Exp. Bot.* **2000**, *51*, 1635−1645.

(17) Howard, B. J.; Beresford, N. A.; Hove, K. Transfer of radiocesium to ruminants in natural and semi-natural ecosystems and appropriate countermeasures. *Health Phys.* **1991**, *61*, 715−725.

(18) Sanchez, A. L.; Wright, S. N.; Smolders, E.; Naylor, C.; Stevens, P. A.; Kennedy, V. H.; Dodd, B. A.; Singleton, D. L.; Barnett, C. L. High plant uptake of radiocesium from organic soils due to Cs mobility and low soil K content. *Environ. Sci. Technol.* **1999**, *33*, 2752−2757.

(19) Veresoglou, D. S.; Tsialtas, J. T.; Barbayiannis, N.; Zalidis, G. C. Cesium and Strontium uptake by two pasture plant species grown in organic and inorganic soils. *Agric., Ecosyst. Environ.* **1995**, *56*, 37−42.

(20) Bryan, N. D.; Robinson, V. J.; Livens, F. R.; Hesketh, N.; Jones, M. N.; Lead, J. R. Metal-humic interactions: A random structural modelling approach. *Geochim. Cosmochim. Acta* **1997**, *61*, 805−820.

(21) Tipping, E.; Hurley, M. A. A unifying model of cation binding by humic substances. *Geochim. Cosmochim. Acta* **1992**, *56*, 3627−3641.

(22) Bryan, N. D.; Jones, D. M.; Appleton, M.; Livens, F. R.; Jones, M. N.; Warwick, P.; Hall, A. A physicochemical model of metal-humate interactions. *Phys. Chem. Chem. Phys.* **2000**, *2*, 1291−1300.

(23) Xu, X.; Kalinichev, A. G.; Kirkpatrick, J. ^{133}Cs and ^{35}Cl NMR spectroscopy and molecular dynamics modeling of Cs^+ and Cl^-

DOI: 10.1021/acs.jpcb.5b01659
J. Phys. Chem. B XXXX, XXX, XXX−XXX

complexation with natural organic matter. *Geochem. Cosmochim. Acta* **2006**, *70*, 4319−4331.
(24) Kalinichev, A. G.; Kirkpatrick, J. Molecular dynamics simulation of cationic complexation with natural organic matter. *Eur. J. Soil. Sci.* **2007**, *58*, 909−917.
(25) Jones, M. N.; Bryan, N. D. Colloidal properties of humic substances. *Adv. Colloid Interface* **1998**, *78*, 1−48.
(26) (a) Leenheer, J. A.; Wershaw, R. L.; Reddy, M. M. Strong acid, carboxyl group structures in fulvic acid from the Suwannee River, Georgia. 1. Minor structures. *Environ. Sci. Technol.* **1995**, *29*, 393−398. (b) Leenheer, J. A.; Wershaw, R. L.; Reddy, M. M. Strong acid, carboxyl group structures in fulvic acid from the Suwannee River, Georgia. 2. Major structures. *Environ. Sci. Technol.* **1995**, *29*, 399−405.
(27) Trout, C. C.; Kubicki, J. D. Deprotonation energies of a model fulvicacid. I. Carboxylicacid groups. *Geochim. Cosmochim. Acta* **2006**, *70*, 44−55.
(28) Trout, C. C.; Kubicki, J. D. Molecular modeling of Al^{3+} and benzene interactions with Suwannee fulvic acid. *Geochem. Cosmochim. Acta* **2007**, *71*, 3859−3871.
(29) Burk, P.; Tammiku-Taul, J.; Tamp, S.; Sikk, L.; Sillar, K.; Mayeux, C.; Gal, J.-F.; Maria, P.-C. Computational Study of Cesium Cation Interactions with Neutral and Anionic Compounds Related to Soil Organic Matter. *J. Phys. Chem. A* **2009**, *113*, 10734−10744.
(30) Mayeux, C.; Gal, J.-F.; Charles, L.; Massi, L.; Maria, P.-C.; Tammiku-Taul, J.; Lohu, E.-L.; Burk, P. A study of the cesium cation bonding to carboxylate anions by the kinetic method and quantum chemical calculations. *J. Mass Spectrom.* **2010**, *45*, 520−527.
(31) Aquino, A. J.; Tunega, D.; Pasalic, H.; Schaumann, G. E.; Haberhauer, G.; Gerzabek, M. H.; Lischka, H. Molecular dynamics simulations of water molecule-bridges in polar domains of humic acids. *Environ. Sci. Technol.* **2011**, *45*, 8411−8419.
(32) Aquino, A. J.; Tunega, D.; Pasalic, H.; Haberhauer, G.; Gerzabek, M. H.; Lischka, H. The thermodynamic stability of hydrogen bonded and cation bridged complexes of humic acid models-A theoretical study. *Chem. Phys.* **2008**, *349*, 69−76.
(33) Aquino, A. J.; Tunega, D.; Schaumann, G. E.; Haberhauer, G.; Gerzabek, M. H.; Lischka, H. Proton transfer processes in polar regions of humic substances initiated by aqueous aluminum cation bridges: A computational study. *Geoderma* **2014**, *213*, 115−123.
(34) Sundararajan, M.; Rajaraman, G.; Ghosh, S. K. Speciation of uranyl ions in fulvic acid and humic acid: a DFT exploration. *Phys. Chem. Chem. Phys.* **2011**, *13*, 18038−18046.
(35) Sinha, V.; Ganguly, B.; Bandyopadhyay, T. Energetics of Ortho-7 (Oxime Drug) Translocation through the Active-Site Gorge of Tabun Conjugated Acetylcholinesterase. *PLoS One* **2012**, *7*, e40188.
(36) Pathak, A. K.; Bandyopadhyay, T. Unbinding free energy of acetylcholinesterase bound oxime drugs along the gorge pathway from metadynamics-umbrella sampling investigation. *Proteins: Struct., Funct., Bioinf.* **2014**, *82*, 1799−1818.
(37) Becke, A. D. Density-functional exchange-energy approximation with correct asymptotic behavior. *Phys. Rev. A* **1988**, *38*, 3098−3100.
(38) Perdew, J. P. Density-functional approximation for the correlation energy of the inhomogeneous electron gas. *Phys. Rev. B* **1986**, *33*, 8822−8824.
(39) Schafer, A.; Horn, H.; Ahlrichs, R. Fully optimized contracted Gaussian basis sets for atoms Li to Kr. *J. Chem. Phys.* **1992**, *97*, 2571−2577.
(40) Sundararajan, M.; Sinha, V.; Bandyopadhyay, T.; Ghosh, S. K. Can functionalized cucurbituril bind actinylcations efficiently? A density functional theory based investigations. *J. Phys. Chem. A* **2012**, *116*, 4388−4395.
(41) Sundararajan, M.; Ganyushin, D.; Ye, S.; Neese, F. Multi-reference Ab initio studies of Zero-Field Splitting and Magnetic Circular Dichroism Spectra of Tetrahedral Co(II) complexes. *Dalton Trans.* **2009**, *30*, 6021−6036.
(42) Sundararajan, M. Quantum Chemical challenges for the binding of Simple Alkanes to Supramolecular hosts. *J. Phys. Chem. B* **2013**, *117*, 13409−13417.
(43) Becke, A. D. Density functional thermochemistry. III. The role of exact exchange. *J. Chem. Phys.* **1993**, *98*, 5648−5682.
(44) Lee, C.; Yang, W.; Parr, R. G. Development of the Colle-Salvetti correlation-energy formula into a functional of the electron density. *Phys. Rev. B* **1988**, *37*, 785−789.
(45) Schafer, A.; Huber, C.; Ahlrichs, R. Fully optimized contracted Gaussian basis sets of triple zeta valence quality for atoms Li to Kr. *J. Chem. Phys.* **1994**, *100*, 5829−5835.
(46) Weigend, F.; Ahlrichs, R. Balanced basis sets of split valence, triple zeta valence and quadruple zeta valence quality for H to Rn: Design and assessment of accuracy. *Phys. Chem. Chem. Phys.* **2005**, *7*, 3297−3305.
(47) Klamt, A.; Schuurmann, G. C. O. S. M. O. COSMO: a new approach to dielectric screening in solvents with explicit expressions for the screening energy and its gradient. *J. Chem. Soc., Perkin Trans.* **1993**, *2*, 799−805.
(48) TURBOMOLE V6.3 2011, a development of University of Karlsruhe and Forschungszentrum Karlsruhe GmbH, 1989−2007, TURBOMOLE GmbH, since 2007; available from http://www.turbomole.com.
(49) Reed, A. E.; Weinstock, R. B.; Weinhold, F. Natural population analysis. *J. Chem. Phys.* **1985**, *83*, 735−746.
(50) Neese, F. *ORCA, Ab Initio Density Functional and Semiempirical Program Package*, version 3.0; Max-Planck-Institute for Chemical EnergyConversion: Ruhr, Germany, 2013.
(51) Hess, B.; Kutzner, C.; van der Spoel, D.; Lindahl, E. GROMACS 4: Algorithms for highly efficient, load-balanced, and scalable molecular simulation. *J. Chem. Theory Comput.* **2008**, *4*, 435−447.
(52) Aqvist, J. J. Ion-water interaction potential derived from free energy perturbation simulations. *J. Phys. Chem.* **1990**, *94*, 8021−8024.
(53) Larentzos, J. P.; Criscenti, L. J. A molecular dynamics study of alkaline earth metal chloride complexation in aqueous solution. *J. Phys. Chem. B* **2008**, *112*, 14243−14250.
(54) Wang, J.; Wang, W.; Kollman, P. A.; Case, D. A. Automatic atom type and bond type perception in molecular mechanical calculations. *J. Mol. Graphics Modell.* **2006**, *25*, 247−260.
(55) Wang, J.; Wolf, R. M.; Caldwell, J. W.; Kollman, P. A.; Case, D. A. Development and testing of a general amber force field. *J. Comput. Chem.* **2004**, *25*, 1157−1174.
(56) Jorgensen, W. L.; Chandrasekhar, J.; Madura, J. D.; Impey, R. W.; Klein, M. L. Comparison of simple potential functions for simulating liquid water. *J. Chem. Phys.* **1983**, *79*, 926−935.
(57) Bussi, G.; Donadio, D.; Parrinello, M. Canonical sampling through velocity rescaling. *J. Chem. Phys.* **2007**, *126*, 014101.
(58) Essmann, U.; Perera, L.; Berkowitz, M. L.; Darden, T.; Lee, H.; Pedersen, L. G. A smooth particle mesh Ewald method. *J. Chem. Phys.* **1995**, *103*, 8577−8593.
(59) Hess, B.; Bekker, H.; Berendsen, H. J. C.; Fraaije, J. G. LINCS: A Linear Constraint Solver for Molecular Simulations. *J. Comput. Chem.* **1997**, *18*, 1463−1472.
(60) Doudou, S.; Vaughan, D. J.; Livens, F. R.; Burton, N. A. Atomistic simulations of calcium uranyl (IV) carbonate adsorption on calcite and stepped-calcite surfaces. *Environ. Sci. Technol.* **2012**, *46*, 7587−7594.
(61) Schlitter, J. Estimation of absolute and relative entropies of macromolecules using the covariance-matrix. *Chem. Phys. Lett.* **1993**, *215*, 617−621.
(62) Laio, A.; Parrinello, M. Escaping free energy minima. *Proc. Natl. Acad. Sci. U. S. A.* **2002**, *99*, 12562−12566.
(63) Laio, A.; Gervasio, F. L. Metadynamics: a method to simulate rare events and reconstruct the free energy in biophysics, chemistry and material science. *Rep. Prog. Phys.* **2008**, *71*, 126601.
(64) Marcus, Y. Thermodynamics of solvation of ions Part 5-Gibbs free energy of hydration at 298.15 K. *J. Chem. Soc., Faraday Trans.* **1991**, *87*, 2995−2999.
(65) Bonomi, M.; Branduardi, D.; Bussi, G.; Camilloni, C.; Provasi, D.; Raiteri, P.; Donadio, D.; Marinelli, F.; Pietrucci, F.; Broglia, R. A.; Parrinello, M. PLUMED: A portable plugin for free-energy

DOI: 10.1021/acs.jpcb.5b01659
J. Phys. Chem. B XXXX, XXX, XXX−XXX

calculations with molecular dynamics. *Comput. Phys. Commun.* **2009**, *180*, 1961−1972.
(66) Caminiti, R.; Musinu, A.; Paschina, G.; Pinna, G. X-ray diffraction study of aqueous SrCl2 solutions. *J. Appl. Crystallogr.* **1982**, *15*, 482−487.
(67) Neilson, G. W.; Broadbent, R. D. The structure of Sr2.in aqueous solution. *Chem. Phys.Lett.* **1990**, *167*, 429−431.
(68) Ohtaki, H.; Radnai, T. Structure and dynamics of hydrated ions. *Chem. Rev.* **1993**, *93*, 1157−1204.
(69) Moreau, G.; Helm, L.; Purans, J.; Merbach, A. E. Structural Investigations of the Aqueous Eu^{2+} Ion: Comparison with Sr^{2+} Using the XAFS Technique. *J. Phys. Chem. A* **2002**, *106*, 3034−3043.
(70) Kerridge, A.; Kaltsoyannis, N. Quantum Chem. Studies of the Hydration of Sr^{2+} in Vacuum and Aqueous Solution. *Chem.—Eur. J.* **2011**, *17*, 5060−5067.
(71) Boda, A.; De, S.; Ali, S. M.; Tulishetti, S.; Khan, S.; Singh, J. K. From Microhydration to bulk hydration of Sr^{2+} metal ion: DFT, MP2 and molecular dynamics study. *J. Mol. Liq.* **2012**, *172*, 110−118.
(72) Ali, Sk. M.; De, S.; Maity, D. K. Microhydration of Cs^+ ion: A density functional theory study on Cs^+-$(H_2O)_n$ clusters (n = 1−10). *J. Chem. Phys.* **2007**, *127*, 044303−11.
(73) Ikeda, T.; Boero, M. Communication: Hydration structure and polarization of heavy alkali ions: A first principles molecular dynamics study of Rb. and Cs^+. *J. Chem. Phys.* **2012**, *137*, 041101.
(74) Schwenk, C. F.; Hofer, T. S.; Rode, B. M. Structure Breaking Effect of Hydrated Cs^+. *J. Phys. Chem. A* **2004**, *108*, 1509−1514.
(75) Chang, R. *Chemistry*; McGraw-Hill: New York, 1994.
(76) Lide, D. R. *CRC Handbook of Chemistry and Physics*; CRC Press: Boca Raton, FL, 2003−2004.
(77) Lumsdon, D. G.; Fraser, A. R. Infrared Spectroscopic Evidence Supporting Heterogeneous Site Binding Models for Humic Substances. *Environ. Sci. Technol.* **2005**, *39*, 6624−6631.
(78) Iskrenova-Tchoukova, E.; Kalinichev, A. G.; Kirkpatrick, R. J. Metal cation complexation with natural organic matter in aqueous solutions: molecular dynamics simulations and potentials of mean force. *Langmuir* **2010**, *26*, 15909−15919.
(79) Samadfam, M.; Niitsu, Y.; Sato, S.; Ohashi, H. Complexation thermodynamics of Sr (II) and humic acid. *Radiochim. Acta* **1996**, *73*, 211−216.
(80) Rusin, P. A.; Quintana, L.; Brainard, J. R.; Strietelmeier, B. A.; Tait, C. D.; Ekberg, S. A.; Clark, D. L. Solubilization of plutonium hydrous oxide by iron-reducing bacteria. *Environ. Sci. Technol.* **1994**, *28*, 1686−1690.
(81) Ashraf, M. A.; Rehman, M. A.; Maah, M. J.; Yusoff, I. Cesium-137: Radio-chemistry, fate and transport, remediation and future concerns. *Crit. Rev. Environ. Sci. Technol.* **2014**, *44*, 1740−1793.
(82) Xiangke, W.; Wenming, D.; Jinzhou, D.; Zuyi, T. Sorption and desorption of radiocesium on calcareous soil: Results from batch and column investigations. J. Radioanal. *Nucl. Chem.* **1999**, *240*, 783−787.
(83) Comans, R. N. J.; Haller, M.; Preter, P. D. Sorption of cesium on Illite: Non-equilibrium behaviour and reversibility. *Geochim. Cosmochim. Acta* **1991**, *55*, 433−440.
(84) van Bergeijk, K. E.; Noordijk, H.; Lembrechts, J.; Frissel, M. J. Influence of pH, soil type and soil organic matter content on soil-to-plant transfer of radiocesium and strontium as analyzed by a nonparametric method. *J. Environ. Radioact.* **1992**, *15*, 265−276.
(85) Lee, M. H.; Lee, C. W. Association of fallout-derived ^{137}Cs, ^{90}Sr and $^{239,240}Pu$ with natural organic substances in soils. *J. Environ. Radioact.* **1999**, *47*, 253−262.
(86) Zhang, M. L.; Ren, A.; Shao, D.; Wang, X. Effect of fulvic acid and ionic strength on the sorption of radiostrontium on Chinese calcareous soil and its solid components. *J. Radioanal. Nucl. Chem.* **2006**, *268*, 33−36.

DOI: 10.1021/acs.jpcb.5b01659
J. Phys. Chem. B XXXX, XXX, XXX−XXX